Laser beam submerged arc hybrid welding: A novel hybrid welding process

Cite as: J. Laser Appl. **30**, 042012 (2018); https://doi.org/10.2351/1.5037269
Submitted: 23 April 2018 • Accepted: 03 October 2018 • Published Online: 21 November 2018

Uwe Reisgen, Simon Olschok and Oliver Engels

Laser beam submerged arc hybrid welding: A novel hybrid welding process

Uwe Reisgen, Simon Olschok, and Oliver Engels
Welding and Joining Institute, RWTH Aachen University, Pontstraße 49, Aachen, North Rhine-Westphalia 52062, Germany

(Received 23 April 2018; accepted for publication 3 October 2018; published 21 November 2018)

The currently predominant joining process for constructional steel in the sheet thickness range of 40 mm, as is customary in pipeline and bridge construction, is submerged arc welding. Due to the large number of welding layers required, a high quantity of energy, expensive welding filler material, and also distortion are introduced into the component. The laser beam submerged arc hybrid welding combines the conventional submerged arc welding process with a high-energy laser beam welding process to form a hybrid process. With this process, sheets with a thickness of up to 40 mm can be joined in butt joints in just two welding layers. In this paper, the hybrid character of this method is emphasized. First, the geometric shape of the melt pool in the cross section is discussed and later the mixing of both melt pools is verified by energy-dispersive x-ray spectroscopy analyses. In addition, results when joining gaps are present are demonstrated and discussed. © *2018 Laser Institute of America*. https://doi.org/10.2351/1.5037269

Key words: laserbeam submerged arc hybrid welding, submerged arc welding, laserbeam welding, hybrid welding

I. INTRODUCTION AND STATE OF THE ART

Joining thick-walled steel structures is a frequently encountered welding task in the field of wind power (foundation and tower structures)[1] or in pipe manufacturing (longitudinal seam and spirally welded pipes).[2] At present, conventional welding processes such as submerged arc welding (SAW) are primarily used to meet this joining task.[1–3] Normally, a double-V-weld seam preparation is selected for this purpose. After some tacking passes have been welded using a gas metal arc welding (GMAW) process, numerous welding beads are welded using the SAW process, depending on the sheet thickness, exemplified by Fig. 1.

It is evident that this involves a great expenditure of time. In addition to the normal welding time, thermal component distortion is almost unavoidable, which means that complex straightening work has to be carried out. Furthermore, large quantities of welding consumables are required. In addition, the high number of welding layers entails the risk of producing intermediate pass errors.[2,5]

Beam welding processes such as laser beam welding (LBW) or electron beam welding provide high-energy densities so that high penetration depths can be achieved with low aspect ratios. Welding time and welding filler material could thus be saved. However, these welding processes require a great deal of time and effort to prepare the weld seam in order to avoid joint gaps, for example. The high cooling rates also often lead to hardening of the weld metal. The combinations of laser welding with conventional GMAW processes to form a hybrid welding gas metal arc-laser arc hybrid welding (GMA-LAHW) process can partially compensate for these disadvantages.[6,7]

Usual laser-arc interdistances (D_{LA})—distance point of impact wire electrode and laser beam—are within the range of 0 (Ref. 8) and 7 mm.[9] With the GMA-LAHW process, penetration depths of up to 20 mm (Ref. 6) and even up to 25 mm (gap with 2.5 mm which is filled up with cut wires and supported by backing)[10] can be achieved with special weld seam preparation. A typical GMA-LAHW weld seam has the shape of a wine glass in the cross section. The upper weld area—dominated by the arc—is significantly wider than the narrow lower weld area—dominated by laser beam (Fig. 2).

A typical welding defect of GMA-LAHW welds is linear defects in the center rib. Especially for double-sided partial penetration, solidification cracks often cannot be avoided.[11,12]

Next to the cracking mentioned in Ref. 13, it is stated that the high cooling rates in combination with high welding penetration depth can lead to remaining pores in the weld seam. Gas bubbles cannot escape over the surface as the melt solidifies. This applies in particular if welding is carried out without complete penetration.[13–15]

As stated by Refs. 16–18, the substitution of the GMAW process by a submerged arc-laser arc hybrid welding (SA-LAHW) process would lead to further increases of the solidification interval of the melt due to the higher energy input. A longer period of time is available for solidification because of slag which covers the molten pool. Degassing is improved so that gas bubbles can escape safely from the root area over the workpiece surface. The process stability, however, is still specified as being too low.[18,19]

Previous investigations have already focused on the combination of laser beam and submerged arc welding processes. However, the results clearly show that there are only two independent and, in this case, separated molten pool areas. This indicates a serial combination of these two welding processes and not a hybrid process. The laser beam merely creates a preheating effect, which leads to an increase in the welding speed for the subsequent submerged arc welding

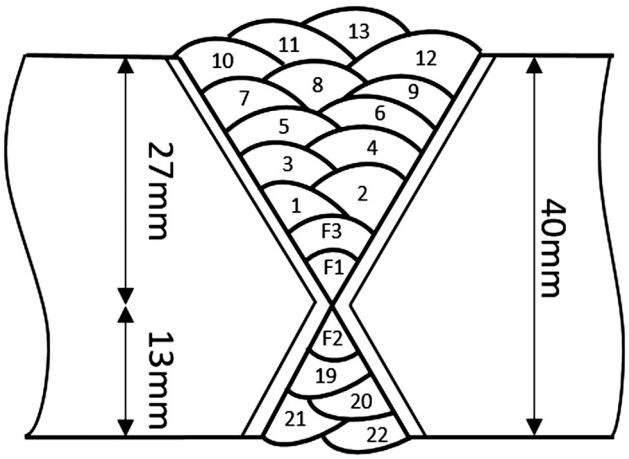

FIG. 1. Conventional edge preparation for 40 mm plate thickness for the SAW process, following Ref. 4.

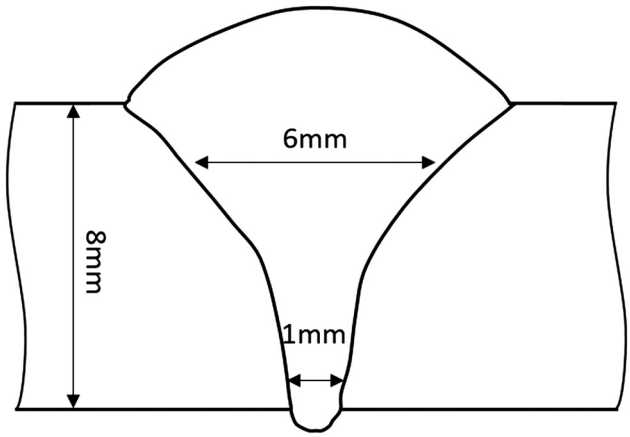

FIG. 2. GMA-LAHW weld seam; schematic.

process.[20,21] Recent research has shown that SA-LAHW joining of sheets with a thickness of 36 and 50 mm with a CO_2 laser or a disk laser for D_{LA} between 32 and 19 mm is possible.[22–25] However, the extent to which this is a standard hybrid welding process was not evaluated in this work.

In the following, welding tests are carried out with the aim of highlighting the hybrid character of the SA-LAHW process. In addition, welding tests are presented which were carried out with preset joining gaps with a maximum width of 2 mm.

II. EXPERIMENTAL SETUP

The basic principle sketch of the SA-LAHW process shows, beside the SAW-torch and the laser beam, also a separating plate which is positioned between the two welding processes (Fig. 3).

The separation plate is used to separate the welding powder necessary for the submerged arc welding process from the effective range of the laser beam. The starting point for the welding tests is a D_{LA} of 15 mm (the distance from the point of impact of the laser beam to the tip of the wire electrode relative to the sheet surface). The angle of incidence of the laser beam optics is 15° to the sheet surface. The inclination angle of the submerged arc welding torch is 3°. The geometrical arrangement of laser and SAW-torch to one another is of great relevance for the welding result and was varied within the scope of the welding results presented in this paper. The welding travel speed is set to 0.6 m/min and the wire feeding rate to 2.1 m/min (these lead to a properly filling degree for this weld seam preparation).

For the welding tests presented below, a structural steel with a yield strength of 355 N/mm² was used. The carbon content is, with 0.033%, very low (Table I). The used submerged arc power source is ESAB (LAE 1250) with a maximum power of 1.250 A. A nickel-containing wire electrode (S2Ni2) with a diameter of 4 mm was used as welding filler material (Table I). The used aluminate-based welding powder has a basicity index according to Boniszewski of 3.2.

The weld seam preparation is carried out as double-Y preparation (depth of root face: 24 mm; total opening angle:

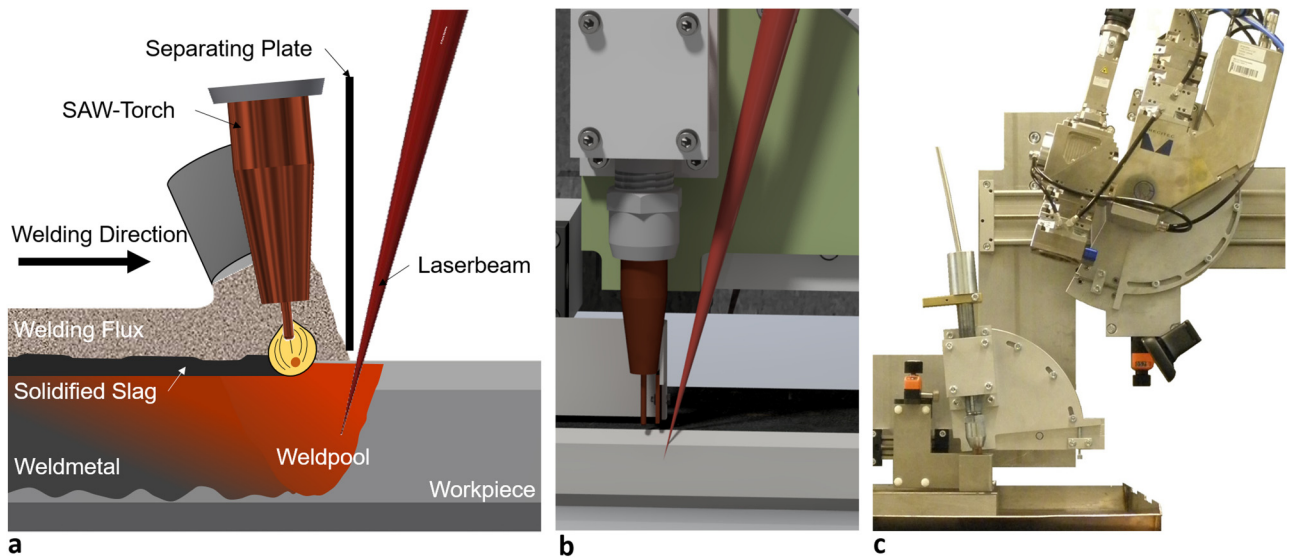

FIG. 3. Welding setup SA-LAHW: process zone schematic (a); process zone computer-aided design model (b); hybrid welding head (c).

TABLE I. Chemical composition (wt. %) of the base material and wire electrode. Balance: iron (Fe).

	C	Si	Mn	P	Cr	Ni	Cu
Base material	0.033	0.33	1.52	0.009	0.15	0.013	0.017
Wire electrode	0.1	0.14	1.02	—	—	2.19	—

70°) (Fig. 4). The sheet thickness is 40 mm. Prior to the welding process, the joining partners were tack welded with the laser beam.

A disk laser from Trumpf (TruDisk 16002) with a maximum output power of 16 kW is used as a laser beam source. The wavelength is 1030 nm and the beam parameter product is 8 mm mrad. The fiber core diameter is 200 μm so that in conjunction with the other beam-forming components, a mathematically determined focal diameter of 0.4 mm results.

In the following, welds are produced which have a process distance of 20 and 15 mm as well as a different angle of incidence of the LBW-optics. In addition, welding tests are presented which were carried out with preset joining gaps with a width of 0, 1, and 2 mm. The welding results were evaluated and discussed by means of macrosections longitudinally and transversally to the welding direction and also by energy-dispersive x-ray spectroscopy (EDX).

III. RESULTS AND DISCUSSION

A. Different process distances

The influence of the laser-arc interdistance and the inclination angle of the LBW-optics on the shaping of the weld seam was investigated. In detail, the inclination angle of the laser beam optics has been changed from 0° to the vertical of the workpiece surface to an angle of 15°, and D_{LA} has been reduced from 20 to 15 mm. Due to the spatial expansion of the SAW-torch, it is not possible to achieve a laser-arc interdistances of less than 20 mm with simultaneous vertical adjustment of the laser beam optics. Therefore, both parameters must be changed at the same time.

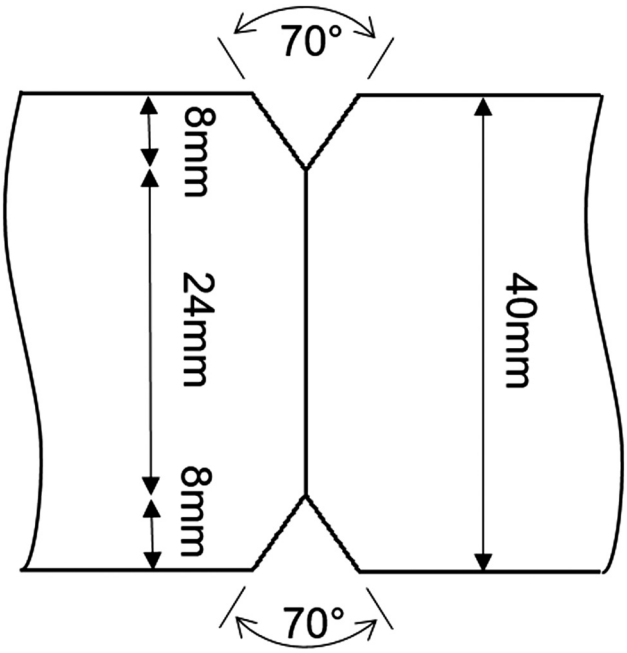

FIG. 4. Weld seam preparation for 40 mm plate thickness for the SA-LAHW process.

The weld seam shown in Fig. 5 was welded with an inclination angle of the LBW-optics of 0° and D_{LA} of

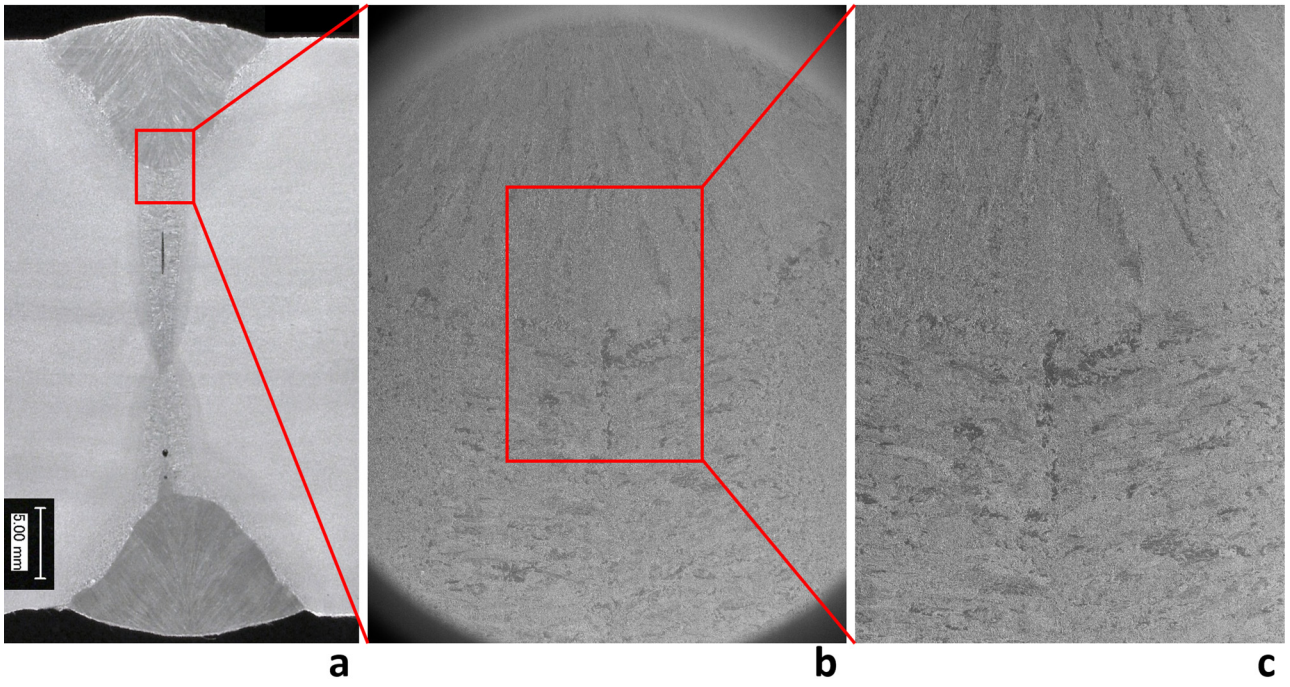

FIG. 5. Cross-sectional SA-LAHW weld seam; $D_{LA} = 20$ mm; macrosection (a); 50× magnification of transition line (b); 70× magnification of transition line (c).

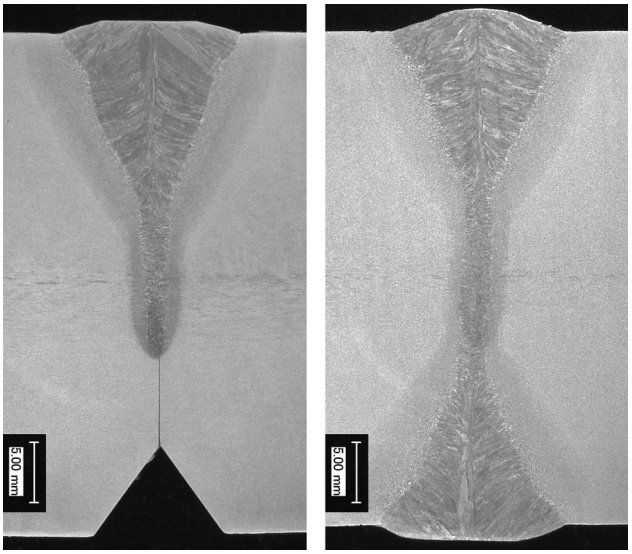

FIG. 6. Cross-sectional SA-LAHW weld seam; $D_{LA} = 15$ mm; pass (a) and counterpass (b).

20 mm. The welding travel speed was 0.6 m/min, the laser beam power was 16 kW, and the wire feed rate was 2.1 m/min. While Fig. 5(a) shows the whole cross section, Figs. 5(b) and 5(c) give a detailed look of the transition area from SAW-dominated to LBW-dominated weld seam area.

The weld seam (Fig. 6) was welded with a 15° inclination angle of the LBW-optics and D_{LA} of 15 mm. Here, the welding travel speed is 0.6 m/min, the beam power is 16 kW, and the wire feed speed is 2.1 m/min.

Although the geometrical shapes of the two shown welding seams are, basically, comparable with those of a GMA-LAHW weld seam (Fig. 2), there are, on some points, significant differences. In terms of quality, the shape of the submerged arc welded area of the weld seam (Fig. 5) can be described as rather flat and wide while the submerged arc welded area of the weld seam (Fig. 6) can be described as rather narrow and deep. Quantitatively, the SAW-dominated weld area of the weld seam (Fig. 5) has a depth of approximately 7.5 mm, whereas the SAW-dominated area of weld seam (Fig. 6) has a depth of approximately 12 mm. When looking at the LBW-dominated weld seam areas, it is noticeable that the LBW area of the right weld seam is narrower and deeper than that of the weld seam (Fig. 5).

In addition, the weld seam (Fig. 5) shows a linear defect in the LBW-dominated weld seam area. Without having examined this defect in detail, it can be assumed that this is the phenomenon of the center rib defect that frequently

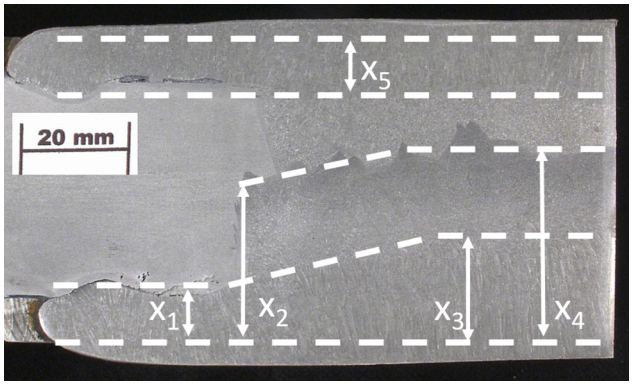

FIG. 7. Longitudinal cross-sectional inlet area SA-LAHW; $D_{LA} = 24$ mm (top); $D_{LA} = 15$ mm (bottom).

occurs during laser welding of large welding depths and which is described in the state of the art.[11–13]

For the weld seam with vertical LBW optic alignment and a D_{LA} of 20 mm (Fig. 5), a total welding depth of approximately 20 mm could be determined. The weld seam with a 15° angle of the LBW-optics and a D_{LA} of 15 mm has a weld penetration depth of 25 mm with otherwise unchanged welding parameters (Fig. 6).

A closer look at the transverse section also reveals that the orientation of dendrite growth in the LBW-dominated weld seam area differs between the two weld seams. The weld seam (Fig. 5) shows a sharp change in orientation at the transition point from the weld seam area dominated by SAW to LBW [Figs. 5(b) and 5(c)]. This may indicate two separate weld seam areas (LBW area solidifies before it is partially remelted by the SAW process). The weld seam (Fig. 6) shows a much wider transition area between the SAW- and LBW-dominated weld seam areas in which the orientation of the dendrites changes continuously. This can indicate the formation of a common weld pool which is the main characteristic of a hybrid welding process.

In addition to the welds discussed here, further welds were performed with a D_{LA} of 15 mm and an angle of incidence of the laser beam optics of 15°. The arc parameters and the beam power were varied to a small extent. Center rib defects as in Fig. 5(a) were not detected in any of them.

In order to substantiate the results discussed in Figs. 5 and 6 using macrosections, double-sided single pass welding was carried out with similar parameters and longitudinal section.

Figure 7 (top) depicts the welding with a D_{LA} of 24 mm and an inclination angle of the LBW-optics of 0°. Figure 7 (bottom) was welded with a D_{LA} of 15 mm and an

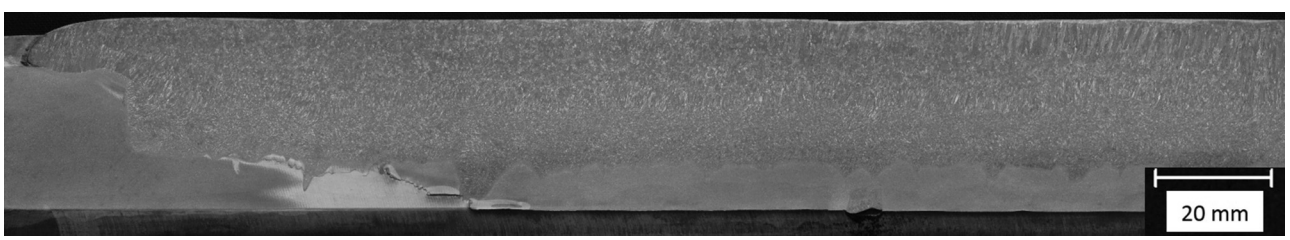

FIG. 8. Longitudinal cross-sectional SA-LAHW; plate thickness 40 mm; effective weld seam length 220 mm; $D_{LA} = 15$ mm.

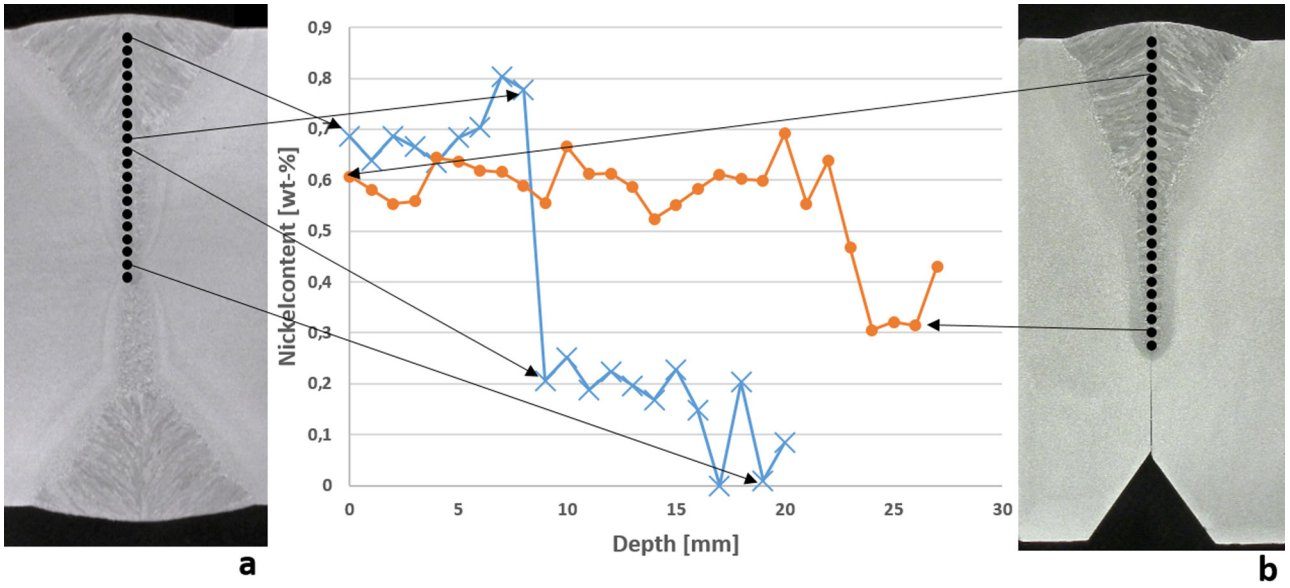

FIG. 9. EDX-analysis along the depth of the weld seam (wt. %); D_{LA} = 15 mm (a) and D_{LA} = 24 mm (b).

inclination angle of the LBW-optics of 15°. The welding travel speed was 0.6 m/min, the laser beam power was 16 kW, and the wire feed rate was 2.1 m/min for both weld seams.

The submerged arc welded area of the upper weld seam has a uniform penetration depth X5 of about 8 mm. The submerged arc welded area of the lower weld seam also has a penetration depth X1 of 8 mm at the start. However, the weld penetration depth increases steadily to about 15 mm as soon as the submerged arc welding process reaches the weld seam area that has already been molten by the laser beam, X3. The increase of the LBW-induced penetration depth is also noticeable. At the start, a welding depth X2 of about 20 mm is achieved. During the running-in process, the weld penetration depth increases steadily to about 25 mm, X4, which supports the assumption that a hybrid welding process has taken place at the weld seam [Fig. 7 (bottom)], and synergy effects have become visible.

With the aim of demonstrating the process stability, a longitudinal section of a weld was made which was welded with a laser-arc interdistance of 15 mm and an inclination angle of 15° (Fig. 8). The welding travel speed was 0.6 m/min, the laser beam power was 16 kW, and the wire feed rate was 2.1 m/min.

The longitudinal section shows that the macrosections discussed in advance are not only a snapshot but also describe the static process behavior. Weld seam defects are not visible. The welding depth is constant over a wide range. The process stability, also during the welding process, can be described as high.

B. Intermixing of the weld pools

As described in the state of the art, there is no complete mixing of the melt pool in the case of large laser-arc interdistances. In further welding tests, chemical test methods were now used to compare the mixing of welding specimens which were welded with a large D_{LA} with those which were welded with a small D_{LA} and inclined laser beam optic. In detail, a weld specimen with a D_{LA} of 24 mm and a vertical laser beam optics as well as a weld specimen with a D_{LA} of 15 mm and a 15° alignment of the laser beam optic were produced. Subsequent to the welding (welding travel speed 0.6 m/min, laser beam power 16 kW, wire feed rate 2.1 m/min), the chemical composition of the weld metal was investigated by means of EDX-analysis, starting from the weld surface in millimeter increments down to the depth of the weld seam. In particular, the concentration of the element nickel introduced by the filler metal and hardly present in the base metal was considered. The results of the EDX-analysis (wt. %) are summarized in Fig. 9.

The weld sample produced with a D_{LA} of 24 mm and an inclination angle of 0° initially has, at the start, a nickel concentration of about 0.7%. From a depth of 8 mm, the nickel concentration suddenly decreases to a value of 0.15%–0.2%. These values are within the range of the detection limit of the measurement method. When looking

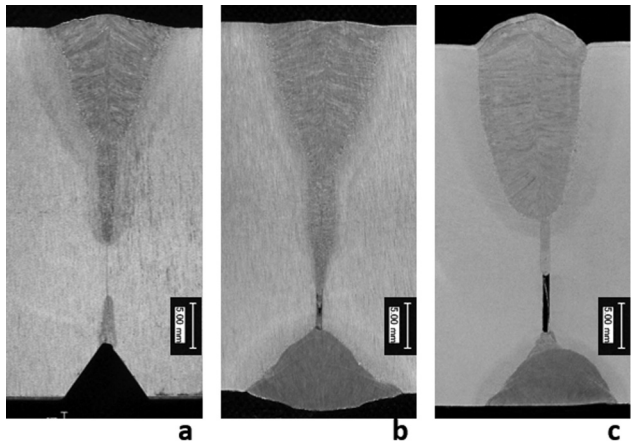

FIG. 10. Cross-sectional SA-LAHW weld seams with gaps; welding travel speed 0.6 m/min; laser beam power 14 kW; gap width 0 mm (a); gap width 1 mm (b); gap width 2 mm (c).

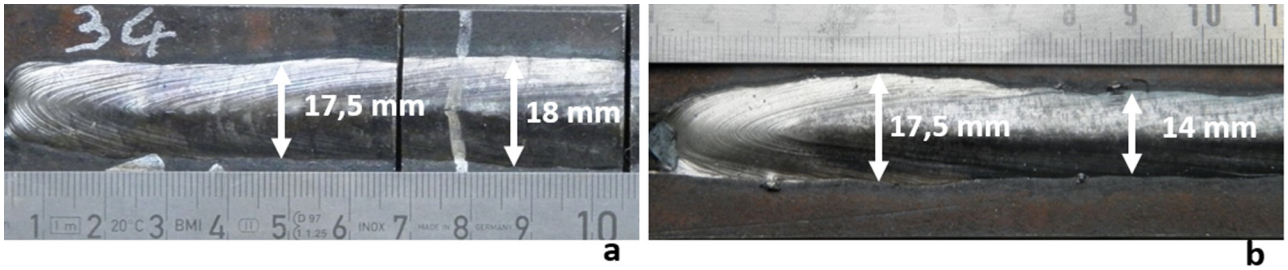

FIG. 11. SA-LAHW weld upper bead, weld start region; $D_{LA} = 20$ mm (a); $D_{LA} = 14$ mm (b).

at the corresponding cross section, it is noticeable that exactly at a depth of 8 mm, the transition point from the SAW-dominated to the LBW-dominated weld seam area can be seen. It can therefore be assumed that the weld area, which is melted by the laser beam, has already solidified before the SAW process reaches this area.

The weld sample with a D_{LA} of 15 mm and an angle of incidence of the laser beam optics of 15° also has a nickel content of approximately 0.6%–0.7% at the start. However, the nickel content in this weld sample only decreases very slightly and, above all, continuously and not abruptly. Even in the LBW-dominated root point of the weld seam at a depth of 25 mm, a nickel content of approximately 0.3% can still be detected. Since the nickel content of the base material is only about 0.015%, it can be assumed that the alloying elements introduced by the filler metal have spread over the entire weld seam area down to the deep root regions. This resulted in a complete mixing of both molten pools. It can therefore be assumed that no solidification has taken place between the two areas.

C. Welding gaps

Furthermore, the robustness of the welding process against the presence of joint gaps was investigated. At a laser-arc interdistance of 15 mm, an adjustment of the LBW-optics to 15°, a laser beam power of 14 kW, and a welding travel speed of 0.6 m/min, joining gaps of 0, 1, and 2 were preset. The wire feed rate was increased from 2.1 m/min (a) over 2.6 m/min (b) to 3.7 m/min (c) (adjusted to properly fill the volume of the gaps). The joining gap was closed with a submerged arc welding process from the opposite side. In addition, beam oscillation (frequency: 100 Hz; amplitude: 1.5 mm) was switched on for the test with a joint gap width of 1 and 2 mm. For these welding trials, the wire electrode was changed to S3Ni1Mo which contains about 0.9 wt. % nickel. Figure 10 shows the welding results in cross section.

Figure 10(a), technical zero gap, shows a typical geometrical shape of the weld pool inside the weld seam. The welding depth is about 22 mm. Figure 10(b), 1 mm joint gap width, shows a comparable geometrical shape of the molten pool. However, the welding depth could be increased to about 26 mm with the same beam power. It can also be seen that the weld seam area dominated by the submerged arc passes very smoothly into the LBW-dominated weld seam area. Figure 10(c), 2 mm joint gap width, shows a completely different geometrical shape compared with the other results. The welding depth is reduced to 19 mm. Below this fusioned depth, there is also material but without any proper fusion to the joint edges (gap-filling sag).[26] Furthermore, no LBW-dominated weld seam area can be detected. The entire weld seam seems to consist of base and deposited material. EDX-measurements over the depth of the weld seam according to the pattern from Fig. 9 showed that there is a homogeneous distribution of the chemical elements in the weld metal for the weld seams with gap width of 1 and 2 mm.

D. Outer shape of the weld seam

In addition to the different geometrical shapes of the weld seam inside the workpiece, there are also conspicuous features visible on the weld upper bead. While keeping the welding travel speed (0.6 m/min), the laser beam power (16 kW), and the wire feed rate (2.1 m/min) constant, the width of the upper bead varies significantly by changing the laser-arc distance. Whereas for welding parameters with large laser-arc interdistances (<20 mm), the weld upper bead has a uniform width of about 18 mm over the entire length of the weld seam [Fig. 11(a)], and two areas can be identified for welds with small laser-arc interdistances (14 mm) [Fig. 11(b)].

The inlet area of the weld seam, i.e., the first 50 mm, has a comparable weld seam width of about 18 mm. Immediately behind the inlet area, the weld seam width is narrowed to

FIG. 12. SA-LAHW weld upper bead: $D_{LA} = 14$ mm; welding travel speed 0.6 m/min; laser beam power 16 kW.

about 14 mm. This width is constant for the whole remaining weld seam. This behavior is always evident when a common molten pool is visible in the weld seam cross section (see Fig. 6) and not two separate weld seam areas (see Fig. 5).

Figure 12 shows the weld upper bead of a weld seam which was welded with a D_{LA} of 14 mm. It can be seen that the weld upper bead has a constant width over the whole length.

IV. CONCLUSION AND OUTLOOK

In this work, it was shown that a hybrid welding process between the laser beam and the submerged arc welding process occurs when the laser beam optics of 15° is inclined in perpendicular to the workpiece and a D_{LA} of 15 mm is set. This was proven by EDX-analyses of the weld metal over the entire depth of the weld seam. At the root point of the weld seam, large portions of the filler metal introduced by the submerged arc welding process can still be detected. With the SA-LAHW process, a laser beam power of 16 kW, a wire feed rate of 2.1 m/min, and a welding speed of 0.6 m/min, penetration depths of about 25 mm can be achieved. Furthermore, welding results were presented which were joined with a preset joining gap. In detail, the joint gap was adjusted up to 2 mm and welded with different feed rates. Quality-conforming welding results were achieved. In addition, conspicuous features on the weld upper bead were highlighted and it was recognized that a constriction of the upper bead width indicates a hybrid welding process.

Further work will focus on the investigation of mechanical and technological properties. Particular emphasis is placed on the homogeneity of those over the entire weld seam area. In addition, the joint gap width will be increased to 3 mm in order to reproduce the tolerances customary in pipe production closer to reality. In addition, GMA-LAHW weld seams are produced and compared with the weld seams produced within this work. For this purpose, the same investigation methods are applied with regard to the intermixing of the filler material in the LBW-dominated weld seam area.

ACKNOWLEDGMENTS

This work was supported by the IGF project "Testing of the laser beam submerged-arc hybrid welding process for industrial applications in the field of large plate thicknesses (LUPuS)," IGF Project No. 19.039 N, of the Research Association for Steel Applications. FOSTA, Düsseldorf, was funded by the AiF within the framework of the programme for the promotion of industrial joint research (IGF) of the Federal Ministry of Economics and Energy on the basis of a decree of the German Bundestag.

[1]K. Hoops and P. Schumacher, "Wirtschaftliche schweißtechnische Produktion von Großkomponenten für Offshore-Windenergieanlagen," in *DVS-Berichte Band 277*, *Schweißen im Schiffbau und Ingenieurbau* (DVS-Media, Duesseldorf, 2011), pp. 47–52.

[2]P. T. Houldcroft, *Submerged-Arc Welding, Woodhead Publishing Series in Welding and Other Joining Technologies* (Woodhead Publishing, Cambridge, 1989), pp. 9–26.

[3]A. Gericke, "Wirtschaftliches UP-Quer-Schweißen an größeren Blechdicken in der Offshorestruktur- und Schiffskörperendmontage," in *DVS-Berichte Band 296*, *Große Schweißtechnische Tagung* (DVS-Verlag, Essen, 2013), pp. 1229–1234.

[4]K.-J. Matthes and E. Richter, *Schweißtechnik - Schweißen von metallischen Konstruktionswerkstoffen*, *Auflage 4* (Carl Hanser Verlag GmbH Co. KG, Muenchen, 2008), pp. 135–137.

[5]U. Reisgen and L. Stein, *Fundamentals of Joining Technologies—Welding, Brazing and Adhesive Bonding* (DVS-Media, Duesseldorf, 2016), pp. 119–132.

[6]F. Vollertsen, M. Rethmeier, A. Gumenyuk, S. Grünewald, U. Reisgen, and S. Olschok, "Welding thick steel plates with fibre lasers and GMAW," Weld. World **54**, 62–70 (2010).

[7]O. Seffer, J. Lindner, A. Springer, S. Kaierle, V. Wesling, and H. Haferkamp, "Laser GMA hybrid welding fort hick wall applications of pipeline steel with the grade X70," in *International Congress on Applications of Lasers and Electro Optics, Anaheim, CA, 2012* (Laser Institute of America, Orlando, 2012), pp. 494–501.

[8]J. Matsuda, A. Utsumi, M. Hamasaki, and S. Nagata, "TIG or MIG arc augmented laser welding of thick mild steel plate," Joining Mater. **1**, 31–34 (1988).

[9]N. Abe, Y. Agamo, M. Tsukamoto, T. Makino, M. Hayashi, and T. Kurosawa, "High speed welding of thick plates using a hybrid-arc combination system," Trans. JWRI **26**, 69–75 (1997).

[10]M. Wahba, M. Mizutani, and S. Katayama, "Single pass hybrid laser-arc welding of 25 mm thick square groove butt joints," Mater. Des. **97**, 1–6 (2016).

[11]M. Schaefer, S. Kessler, P. Scheible, N. Speker, and T. Harrer, "Hot cracking during laser welding of steel: Influence of the welding parameters and prevention of cracks," Proc. SPIE **10097**, 100970E (2017).

[12]F. Farrokhi, S. E. Nielsen, R. H. Schmidt, S. S. Pedersen, and M. Kristiansen, "Effect of cut quality on hybrid laser arc welding of thick section steels," Phys. Procedia **78**, 65–73 (2015).

[13]U. Dilthey, K. Woeste, and S. Olschok, "Modern beam-welding technologies in advanced pipe manufacturing," *4th European Conference on Steel and Composite Structures, Eurosteel, Netherlands, 2005* (Druck und Verlagshaus Mainz, Aachen, 2005), pp. 2.2–9.

[14]K. Seiji, N. Yasuaki, U. Satoru, and M. Masami, "Physical phenomena porosity mechanism in laser-arc hybrid welding," Trans. JWRI **35**, 13–18 (2006).

[15]A. Kaplan, M. Mizutani, S. Katayama, and A. Matsunawa, "First international symposium on high-power laser macroprocessing," Proc. SPIE **4831**, 1–6 (2003).

[16]U. Dilthey and S. Olschok, Abschlussbericht des AiF-Forschungsvorhabens 13.407 N, 2004.

[17]U. Reisgen and S. Olschok, "Laser-submerged arc hybrid welding," Paton Weld. J. **4**, 38 (2009).

[18]U. Dilthey, K. Woeste, and S. Olschok, in *Conference Report: Eurosteel* (Druck und Verlagshaus Mainz, Aachen, 2005).

[19]P. Kah, "Overview of the exploration status of laser-arc hybrid welding processes," Rev. Adv. Mater. Sci. **30**, 120–121 (2012).

[20]J. C. Coiffier, J. P. Jansen, G. Peru, and J. Claeys, "Combination of laser beam and submerged arc processes for the longitudinal welding of large welded pipes," in *International Symposium of High Strength Steels, Trondheim, Norway, 1–2 July 1997.*

[21]I. Krivtsun and P. Seyffarth, *Laser Arc Processes and Their Applications in Welding and Material Treatment* (Taylor & Francis, London, 2002).

[22]U. Reisgen, S. Olschok, S. Jakobs, M. Schleser, O. Mokrov, and E. Rossiter, "Laser beam submerged arc hybrid welding," Phys. Procedia **39**, 75–83 (2012).

[23]U. Reisgen, S. Olschok, and S. Jakobs, "Laser submerged arc hybrid welding (LUPuS) with solid state lasers," Phys. Procedia **56**, 653–662 (2014).

[24]U. Reisgen, S. Olschok, S. Jakobs, and O. Engels, "Modern hybrid welding process for structural steelwork engineering—Laser submerged arc hybrid welding," J. Laser Appl. **28**, 022011 (2016).

[25]U. Reisgen, S. Olschok, and O. Engels, "Innovative hybrid welding process for structural steelwork engineering—Laser submerged arc hybrid welding," J. Laser Appl. **29**, 022401 (2017).

[26]I. Bunaziv, J. Frostevarg, O. M. Akselsen, and A. F. H. Kaplan, "The penetration efficiency of thick plate laser-arc hybrid welding," Int. J. Adv. Manuf. Technol. **97**, 2907–2919 (2018).